Matrix stiffening promotes a tumor vasculature phenotype

Francois Bordeleau[a,1], Brooke N. Mason[a,1], Emmanuel Macklin Lollis[b], Michael Mazzola[a], Matthew R. Zanotelli[a], Sahana Somasegar[a], Joseph P. Califano[a], Christine Montague[a], Danielle J. LaValley[a], John Huynh[a], Nuria Mencia-Trinchant[c], Yashira L. Negrón Abril[d], Duane C. Hassane[c], Lawrence J. Bonassar[a,e], Jonathan T. Butcher[a], Robert S. Weiss[d], and Cynthia A. Reinhart-King[a,2]

[a]Nancy E. and Peter C. Meinig School of Biomedical Engineering, Cornell University, Ithaca, NY 14853; [b]Robert Frederick Smith School of Chemical and Biomolecular Engineering, Cornell University, Ithaca, NY 14853; [c]Division of Hematology and Medical Oncology, Department of Medicine, Weill Cornell Medical College, New York, NY 10065; [d]Biomedical Sciences, Cornell University, Ithaca, NY 14853; and [e]Sibley School of Mechanical and Aerospace Engineering, Cornell University, Ithaca, NY 14853

Edited by Lance L. Munn, Massachusetts General Hospital and Harvard Medical School, Charlestown, MA, and accepted by Editorial Board Member Rakesh K. Jain December 2, 2016 (received for review August 23, 2016)

Tumor microvasculature tends to be malformed, more permeable, and more tortuous than vessels in healthy tissue, effects that have been largely attributed to up-regulated VEGF expression. However, tumor tissue tends to stiffen during solid tumor progression, and tissue stiffness is known to alter cell behaviors including proliferation, migration, and cell–cell adhesion, which are all requisite for angiogenesis. Using in vitro, in vivo, and *ex ovo* models, we investigated the effects of matrix stiffness on vessel growth and integrity during angiogenesis. Our data indicate that angiogenic outgrowth, invasion, and neovessel branching increase with matrix cross-linking. These effects are caused by increased matrix stiffness independent of matrix density, because increased matrix density results in decreased angiogenesis. Notably, matrix stiffness up-regulates matrix metalloproteinase (MMP) activity, and inhibiting MMPs significantly reduces angiogenic outgrowth in stiffer cross-linked gels. To investigate the functional significance of altered endothelial cell behavior in response to matrix stiffness, we measured endothelial cell barrier function on substrates mimicking the stiffness of healthy and tumor tissue. Our data indicate that barrier function is impaired and the localization of vascular endothelial cadherin is altered as function of matrix stiffness. These results demonstrate that matrix stiffness, separately from matrix density, can alter vascular growth and integrity, mimicking the changes that exist in tumor vasculature. These data suggest that therapeutically targeting tumor stiffness or the endothelial cell response to tumor stiffening may help restore vessel structure, minimize metastasis, and aid in drug delivery.

tumor stiffness | endothelial cells | vascular permeability | glycation | extracellular matrix

The ingrowth of newly sprouted blood vessels is necessary for solid tumor growth, and tumor vasculature is typically malformed, leakier, and more tortuous than the vasculature of normal tissues (1–3). Generally, aberrant tumor vasculature is considered to be caused by up-regulated VEGF expression resulting in chaotic vascular growth and failure to establish mature, well-regulated networks (4, 5). Here, we propose a different hypothesis, namely that extracellular matrix (ECM) mechanical properties also contribute to the aberrant vascular phenotype seen in tumors.

Solid tumor tissue is typically stiffer than native, healthy tissue (1, 6). Increased ECM stiffness within tumors is caused primarily by both increased collagen deposition and increased cross-linking within the tumor stroma (7). Increased ECM density and cross-linking are associated with poor prognosis in a number of cancers (8, 9). Many studies have investigated the role of matrix density on angiogenesis and, in both collagen and fibrin matrices, have shown that angiogenesis decreases with increasing matrix concentration (10–13). Increased matrix density appears to act as a physical barrier that restricts cell migration, and cells rely on matrix metalloproteinases (MMPs) to overcome that barrier (14, 15). Indeed, evidence points to an important role of MMP regulation in efficient angiogenesis (16, 17). Most notably, membrane-type matrix metalloproteinase 1 (MT1-MMP) appears to play a central role in regulating tumor-associated angiogenesis and vascular function (18). However, within the tumor microenvironment, ECM stiffness can increase independently of collagen density through cross-linking enzymes (7). Cross-linking can result in increased matrix stiffness without changing the ECM architecture (19). Recent work has shown that endothelial cells (ECs) are mechanosensitive to changes in matrix stiffness (20, 21), but matrix stiffening in the tumor microenvironment affects tumor angiogenesis remains less clear.

In this study, we examine the effects of collagen cross-linking and the resulting increase in matrix stiffness on the growth and integrity of angiogenic vessels. Using in vitro, in vivo, and *ex ovo* models, we show that increasing the extent of collagen cross-linking leads to significantly more vessel outgrowth and branching. We further show that matrix stiffness plays an important role in vessel permeability and endothelial cell–cell junctional integrity. Together, our results demonstrate that matrix cross-linking modulates the growth, structure, and integrity of neo-vessels and suggest that the phenotype of tumor vasculature is mediated in part by collagen cross-linking.

Significance

Dysregulation of both vascular architecture and function is a hallmark of numerous diseases, including cancer. This dysregulation is currently largely attributed to up-regulated proangiogenic growth factors. Here, we show that the stiffness of the underlying extracellular matrix also plays a central role in promoting angiogenesis and a characteristic tumor-like vasculature both in vitro and in vivo. The matrix stiffness-mediated angiogenesis is dependent on increased matrix metalloprotease activity. In addition, increased matrix cross-linking disrupts endothelial cell–cell junctional integrity and results in leakier vasculature. These results suggest that altered tissue mechanics, which are characteristic of solid tumors, directly influence vascular phenotype and, subsequently, may impair therapeutic delivery and efficacy.

Author contributions: F.B., B.N.M., D.J.L., D.C.H., L.J.B., J.T.B., R.S.W., and C.A.R.-K. designed research; F.B., B.N.M., E.M.L., M.M., M.R.Z., S.S., J.P.C., C.M., J.H., N.M.-T., Y.L.N.A., and D.C.H. performed research; F.B., B.N.M., E.M.L., M.R.Z., S.S., J.P.C., C.M., D.J.L., J.H., and D.C.H. analyzed data; and F.B., B.N.M., E.M.L., D.C.H., and C.A.R.-K. wrote the paper.

The authors declare no conflict of interest.

This article is a PNAS Direct Submission. L.L.M. is a Guest Editor invited by the Editorial Board.

Freely available online through the PNAS open access option.

[1]F.B. and B.N.M. contributed equally to this article.

[2]To whom correspondence should be addressed. Email: cak57@cornell.edu.

This article contains supporting information online at www.pnas.org/lookup/suppl/doi:10.1073/pnas.1613855114/-/DCSupplemental.

Results

Collagen Cross-Linking and Collagen Density Modulate the Mechanical Properties and Fiber Arrangements of Collagen Gels. To establish an in vitro model in which collagen stiffness can be modulated, the individual and combined effects of collagen cross-linking and collagen density on the mechanical and structural properties of collagen gels were studied. Cross-linking of collagen was done through nonenzymatic glycation to form advanced glycation end product (AGE) cross-links (19), followed by confined compression testing to characterize the mechanical properties of the collagen gels. Increasing the density of the collagen gels from 1.5 to 10 mg/mL increases the equilibrium compressive modulus approximately sixfold, from ∼180 to ∼1,200 Pa (Fig. 1*A*). Within a given density, increasing the extent of glycation from 0 to 100 mM also increases the modulus of the gels from ∼180 to ∼500 Pa, ∼600 to ∼715 Pa, and ∼1,200 to ∼1,400 Pa for 1.5-, 5-, and 10-mg/mL collagen gels, respectively. To investigate the effects of collagen density and cross-linking on collagen gel fiber architecture further, the internal collagen fiber distributions were visualized with confocal reflectance microscopy. Increasing the density of the collagen visibly decreases the porosity and alters the size and distribution of fibers within the collagen gels (Fig. S1). However, collagen gels within a given density and glycated with 0, 50, or 100 mM ribose form gels with qualitatively similar fiber architectures. Taken together, these results indicate that nonenzymatic glycation can modulate the mechanical properties of collagen gels while only minimally altering the collagen fiber architecture.

Angiogenic Outgrowth and Branching Are Modulated by ECM Mechanical Properties. The effects of stiffening collagen gels via either cross-linking through glycation or increased density on EC migration and outgrowth were investigated. Interestingly, single-cell 3D migration speed decreased and the persistence time increased as the stiffness of the gels increased (Fig. 1 *B* and *C*). Increasing the density of the collagen matrix decreased the overall outgrowth of angiogenic sprouts from the spheroids (Fig. S2), as has been shown previously (11). Importantly, however, at all densities, increasing the stiffness of the collagen via glycation increased the outgrowth response from the spheroids. EC spheroids invaded significantly farther in collagen gels glycated with 100 mM ribose than with 0 mM ribose beginning at days 1 and 3 for 1.5-mg/mL and 5-mg/mL collagen densities, respectively (Fig. 1*D*). This trend is observed across all collagen densities, although it is not statistically significant at 10 mg/mL. However, there were significantly more angiogenic sprouts in glycated gels at all densities (Fig. 1*E*). These findings suggest that the effects of stiffness on EC sprouting are dependent on the mechanism of stiffening, i.e., cross-linking or increased density.

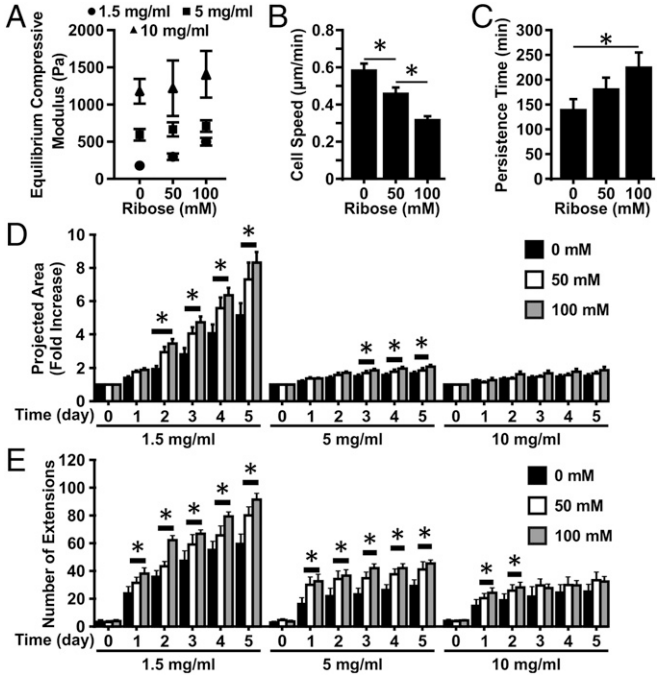

Fig. 1. Matrix density and cross-linking alter collagen gel mechanical properties and the angiogenic sprouting response from multicellular spheroids. (*A*) Equilibrium compressive moduli of 1-, 5-, and 10-mg/mL collagen gel following cross-linking with 0, 50, or 100 mM ribose. (*B* and *C*) Quantification of migration speed (*B*) and persistence (*C*) for ECs embedded within 1.5-mg/mL collagen gels glycated with 0, 50, or 100 mM ribose. (*D* and *E*) The projected spheroid area (*D*) and the number of extensions (*E*) were measured over the course of 5 d. Data are presented as mean ± SEM; $*P < 0.05$.

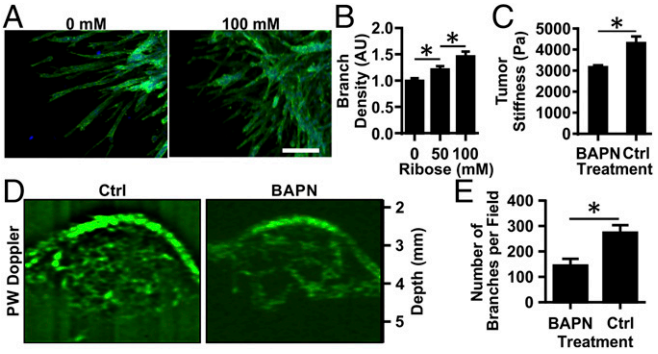

Fig. 2. Matrix cross-linking alters angiogenic branching in vitro and in vivo. EC multicellular spheroids were embedded within 1.5-mg/mL collagen gels glycated with 0, 50, or 100 mM ribose. (*A*) Spheroids were fixed, stained for actin (green) and nuclei (blue), and imaged using confocal microscopy after 5 d. (Scale bar, 100 μm.) (*B*) The number of branches per sprout length was counted, and data were normalized to the 0-mM ribose condition. AU, arbitrary units. (*C*) MMTV-PyMT mice were treated with BAPN to prevent collagen cross-linking or with vehicle (controls; Ctrl), and the equilibrium compressive moduli were measured using unconfined compression testing. (*D*) The tumor vasculature was visualized using ultrasound. (*E*) The number of visible vascular branches was quantified using the ImageJ Tubeness plugin. Data are presented as mean + SEM; $*P < 0.05$.

Notably, tumor angiogenesis is marked by increased branching and tortuosity (5). Our previous work indicates that matrix cross-linking alters the shape of individual cells (19), suggesting it also may alter the shape of assemblies of cells during angiogenesis. To analyze further the effects of matrix stiffness on the shape and structure of neovessels, the density of branching along vessels outgrowths was analyzed. Increasing the stiffness of the gels via nonenzymatic glycation increased the density of branching in angiogenic outgrowths from spheroids (Fig. 2*A*). Outgrowths from spheroids in stiffer gels (100 mM ribose) had an ∼1.5-fold increase in branching compared with those within more compliant (0 mM ribose) gels (Fig. 2*B*). These findings indicate that increasing matrix stiffness via cross-linking not only causes increased outgrowth from spheroids but also changes the morphology of the angiogenic sprouts that form, mimicking the changes occurring in the tumor microenvironment.

Given our in vitro findings, we speculated that tumor angiogenesis is mediated in part by the matrix cross-linking that occurs in the tumor microenvironment. To investigate the relationship between tissue stiffness and tumor angiogenesis, we extended our analysis to the MMTV-PyMT mouse tumor model (6, 22). To modulate the stiffness of the spontaneous mammary tumors that develop in these mice, we used β-aminopropionitrile (BAPN), an inhibitor of the matrix cross-linking enzyme lysyl oxidase (LOX) involved in tumor stiffening (Fig. 2*C*) (6, 23). BAPN is a commonly used model to interrogate the mechanical properties of the ECM

in tumor physiology and enables the examination of the effects of matrix cross-linking on angiogenesis when cross-linking is modulated by inhibition of LOX (6, 22). Ultrasound power wave Doppler was used to image the extensive vasculature within PyMT mouse tumors (Fig. 2*D*, Fig. S3*A* and Movie S1). The vasculature in BAPN-treated mice, in which tumor stiffness is decreased, was far less prominent (Fig. 2*D*, Fig. S3*A*, and Movie S2). Quantification of the vascular network indicates that the number of branches and junctional nodes within the vascular network is significantly reduced in mice treated with BAPN compared with the vehicle control treatment (Fig. 2*E* and Fig. S3*B*). Overall, reducing tumor stiffness by decreasing collagen cross-linking with BAPN reduced the extent of angiogenesis within the tumor.

Given our in vivo results showing increased angiogenesis in cross-linked matrices, we extended our analysis to an *ex ovo* chick chorioallantoic membrane (CAM) angiogenesis assay. Collagen implants containing 5 μg/mL VEGF were placed on the distal region of the CAM on embryonic day (E) 10 (Fig. S4*A*). A VEGF ELISA was used to examine the release profile of VEGF to confirm that VEGF release is not affected by the stiffness of the gels (Fig. S4*B*). On E15, vessels within the collagen gels were imaged using confocal microscopy and appeared as thin fluorescent sprouts (Fig. 3*A*, arrowheads). Stiffer collagen gels (100 mM ribose) promoted significantly more angiogenesis than the more compliant (0 mM ribose) gels (Fig. 3*B*). These data support our in vitro and in vivo findings that matrix stiffness resulting from cross-linking enhances angiogenesis.

Stiffness-Mediated Angiogenic Outgrowth Requires MMP Activity. Because prior work suggests that MMP activity plays a key role in cell migration in response to increased matrix density (11, 15), we hypothesized it may serve a similar function in mediating angiogenesis in response to increased matrix cross-linking. Toward that end, we assayed for the expression and activity of the MT1-MMP in ECs in 3D cell culture because of its role in regulating tumor vasculature (18). Both MT1-MMP expression and activity, as revealed by the presence of the cleaved fragment, were increased in the stiffer gels (100 mM ribose) compared with the more compliant gels (0 mM ribose) (Fig. 4*A*). Treatment with the MMP inhibitor GM6001 blocked MT1-MMP cleavage in both conditions. Using a specific MT1-MMP activity probe, we confirmed that MT1-MMP activity was indeed increased in stiffer gels (Fig. 4*B*). Similar to observations in epithelial cells (24), the stiffness-mediated increase in EC MT1-MMP activity is dependent on Rho-associated protein kinase (ROCK)-mediated cell contractility (Fig. 4*B*). However, we did not observe any significant changes in MT1-MMP mRNA content in the gels of different stiffness (Fig. 4*C*) or any significant differences in content in vivo (Fig. S5). We then examined spheroid outgrowth when MMPs were inhibited using GM6001. Spheroids in stiffer gels (100 mM ribose) had significantly less angiogenic outgrowth in the presence of 5 μM GM6001 than did untreated control cells in the same matrix (Fig. 4 *B* and *C*); the spheroid outgrowth was similar within the more compliant gels (0 mM ribose) with or without GM6001 treatment. In all conditions, the morphologies of angiogenic sprouts were altered with GM6001 treatment (Fig. 4*D*). Sprouts in compliant and stiff control gels (0 and 100 mM ribose) had similar morphologies, whereas sprouts from spheroids cultured with GM6001 were much thinner than controls (Fig. 4*E*). Moreover, stiffness-mediated angiogenic outgrowth in the CAM angiogenesis assay was prevented upon MMP inhibition (Fig. 4*F*). These data suggest that MMPs play an important role in promoting the increased angiogenesis observed in stiffer matrices.

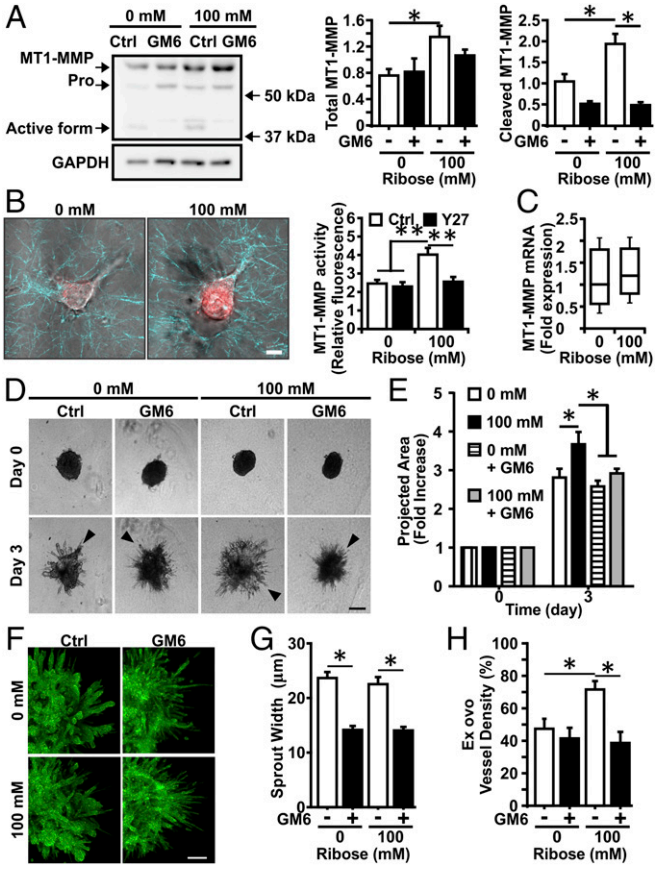

Fig. 4. Stiffness-mediated angiogenic outgrowth requires MMP activity. (*A*, *Left*) Western blot for MT1-MMP in ECs embedded within 1.5-mg/mL collagen gels glycated with 0 or 100 mM ribose and fed with complete medium with (GM6) or without (Ctrl) 5 μM GM6001. (*Right*) The corresponding densitometric quantification normalized to actin content. GAPDH was used as loading control. (*B*, *Left*) Confocal images showing MT1-MMP activity in ECs embedded within 1.5-mg/mL collagen gels glycated with 0 or 100 mM ribose. (*Right*) The corresponding quantification with (Y27) or without (Ctrl) 10 μM of the ROCK inhibitor Y27632. (Scale bar, 10 μm.) (*C*) MT1-MMP expression determined by quantitative real-time RT-PCR does not show expression differences as a function of increased stiffness. (*D*) EC multicellular spheroids were embedded within 1.5-mg/mL collagen gels glycated with 0 or 100 mM ribose and fed with complete medium with (GM6) or without (Ctrl) 5 μM GM6001. (Scale bar, 200 μm.) (*E*) Spheroid outgrowth was quantified after 3 d of culture and normalized to the day 0 condition. (*F*) Spheroids were stained for actin (green) and nuclei (blue) and were imaged with confocal microscopy. (Scale bar, 100 μm.) (*G*) The width of angiogenic sprouts was measured by fitting the intensity profile of a line drawn perpendicular to the sprout with a two-Gaussian curve. (*H*) Quantification of vessel density into 1.5-mg/mL collagen gels glycated with 0 or 100 mM ribose during the CAM angiogenic sprouting assay with or without 5 μM GM6001. Data are presented as mean + SEM; $*P < 0.05$.

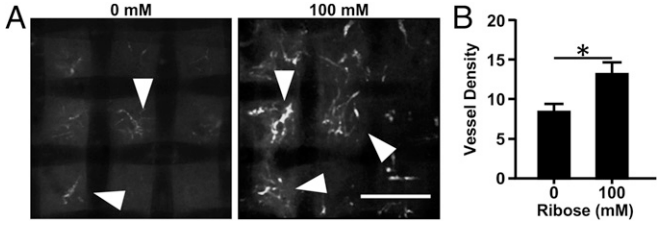

Fig. 3. Matrix cross-linking alters angiogenic sprouting into collagen gels in the chick CAM model. Angiogenic sprouting (arrowheads) into 1.5-mg/mL collagen gels glycated with 0 or 100 mM ribose were imaged with confocal microscopy (*A*), and the vessel density per gel was quantified (*B*). (Scale bar, 200 μm.) Data are presented as mean + SEM; $*P < 0.05$.

Matrix Stiffness Influences the Localization of Vascular Endothelial Cadherin and Barrier Integrity. We next sought to investigate the functional integrity of newly formed vessels as a function of matrix stiffness. Importantly, increased vessel permeability is a hallmark of

tumor vasculature (2, 25). Our previous data indicate that increased matrix stiffness disrupts cell–cell junctions (20, 21, 26), suggesting that stiffness may result in impaired barrier integrity. Vascular endothelial cadherin (VE-cadherin) within EC–EC junctions in vascular sprouts was imaged as a function of stiffness (Fig. 5*A*). We found that the VE-cadherin junctions within the stiff (100 mM ribose) collagen were significantly wider than those within the more compliant (0 or 50 mM ribose) collagen gels (Fig. 5*B*).

Our previous data suggest that subconfluent ECs on compliant substrates assemble spontaneously into networks reminiscent of the angiogenic process (27). Using this 2D platform, which is more amenable to imaging and manipulation than 3D cultures, we extended our analysis of VE-cadherin to EC cultured on compliant (0.2 kPa) or stiff (10 kPa) polyacrylamide (PA) substrates to visualize and characterize its localization better. Cells on compliant substrates formed VE-cadherin– and β-catenin–positive EC–EC junctions that were continuous between cells, whereas the junctions on stiff substrates were punctate (Fig. 5*C*). The tight junction protein zona occludens 1 (ZO-1) shows stiffness-mediated localization that matches with VE-cadherin localization (Fig. S6*A*). In vivo staining of VE-cadherin, ZO-1, and β-catenin further revealed changes in junction architecture in stiffer tumors (Fig. S6 *B* and *C*). Cytoskeletal fractionation of cell lysate from ECs indicates that significantly greater proportions of total VE-cadherin, β-catenin, and γ-catenin content were found in the Triton-insoluble fraction in ECs plated on compliant gels than in ECs plated on the gels (Fig. 5*D*). Junction proteins of ECs embedded within glycated 3D collagen gels presented a similar stiffness-mediated insoluble/soluble dependence (Fig. 5*E*).

We further proceeded to investigate the effects of matrix stiffness and altered VE-cadherin localization on ECs barrier integrity. Because AGEs are found in tumors (28, 29) and have been shown before to perturb EC barrier integrity (30), we proceeded to evaluate the permeability of EC monolayers on glycated collagen-coated PA gels of varying stiffness. Although increasing the matrix stiffness significantly increased the permeability of EC monolayers, the extent of collagen glycation had no significant effect (Fig. 5 *F* and *G*), suggesting that increased permeability is

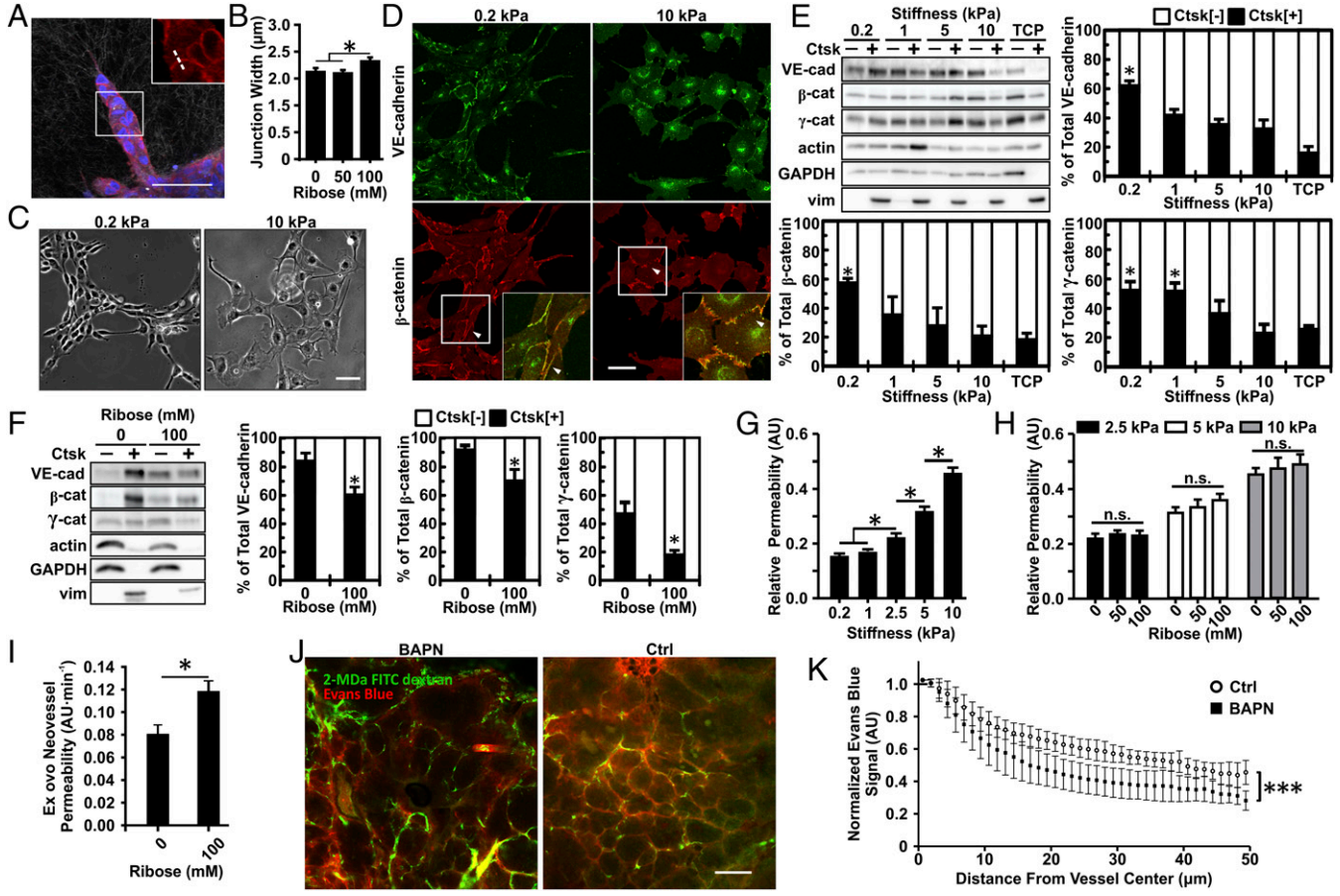

Fig. 5. Matrix stiffness alters VE-cadherin expression, junction width, and endothelial cell permeability. (*A*) EC spheroids were fixed 24 h after embedding within 1.5-mg/mL collagen gels glycated with 0, 50, or 100 mM ribose and were imaged with confocal microscopy to visualize VE-cadherin (red) and nuclei (blue) with confocal reflectance of the collagen fibers. The zoomed-in insert shows a representative region used to obtain the VE-cadherin junction width profiles from a line perpendicular to the junction (dotted line). (*B*) Corresponding quantification of the width of junctions between stalk cells of the sprouts. (*C* and *D*) Phase-contrast images showing ECs seeded on compliant (0.2 kPa) or stiff (10 kPa) PA substrates (*C*) along with the corresponding VE-cadherin and β-catenin localization at cell–cell junctions (arrowheads) showing a continuous distribution on compliant matrix and a punctate distribution on stiff matrix (*D*). *Insets* are magnifications of boxed regions. (*E* and *F*) Western blot and corresponding quantification of VE-cadherin, β-catenin, and γ-catenin content in the soluble fraction (Ctsk[−]) versus the cytoskeleton-associated insoluble fraction (Ctsk[+]) for ECs seeded on PA 2D substrate (*E*) or ECs embedded within 1.5-mg/mL collagen gels glycated with 0 or 100 mM ribose (*F*). Vimentin was used as the insoluble Ctsk[+] fraction control. TCP, tissue culture plastic. (*G* and *H*) Quantification of the EC monolayer permeability to 40-kDa FITC-dextran in response to matrix stiffness (*G*) and collagen glycation (*H*). (*I*) Quantification of the neovessel permeability in the CAM angiogenic sprouting assay in 1.5-mg/mL collagen gels glycated with 0 or 100 mM ribose. (*J*) Representative confocal images from MMTV-PyMT mice treated with BAPN or vehicle controls (Ctrl) showing 2-MDa FITC-dextran–labeled vasculature (green) and extravasating Evans blue (red). (*K*) Quantification of vessel permeability to Evans blue with BAPN or vehicle controls (Ctrl). (Scale bars, 50 μm.) Data are presented as mean ± SEM; $*P < 0.05$, $***P < 0.0001$.

caused by matrix stiffness, not by EC interaction with AGEs. Moreover, we observed an increase in vessel permeability as a function of stiffness using the CAM angiogenesis assay (Fig. 5*H*). We then extended our analysis to the BAPN-treated MMTV-PyMT mouse tumor model, using an in vivo Evans blue extravasation assay to confirm our in vitro permeability findings. Notably, the higher matrix stiffness found in control mice disrupts EC barrier function of the tumor-associated vasculature to a greater extent than in the BAPN-treated mice (Fig. 5 *I* and *J* and Fig. S7). Of note, we did not observe any BAPN-mediated effects on EC permeability or mRNA expression in vitro, suggesting that BAPN does not affect EC integrity directly (Fig. S8). Together, these data indicate that the stiffness of the matrix modulates the integrity of VE-cadherin junctions, with stiff substrates preventing strong cell–cell adhesion and disrupting barrier integrity.

Discussion

Matrix cross-linking is one of the main mechanisms by which the tumor stroma stiffens during solid tumor progression (6, 7). Although several studies have investigated the role of increasing 3D matrix stiffness via matrix density on angiogenesis (10–13), much less is known about the role of cross-linking on the formation of vascular structures. Here, we modulated matrix stiffness by increasing the extent of cross-linking through nonenzymatic glycation. We show that increasing matrix cross-linking increased the extent of outgrowth and branching in endothelial spheroids, in vivo mouse tumors, and in an *ex ovo* embryonic chick model. We demonstrate that endothelial cell–cell junctional properties are modulated by the stiffness of the matrix and that the localization of VE-cadherin and the permeability of endothelial monolayers are significantly altered by matrix stiffness. We also show that inhibiting MMP activity prevents the increased outgrowth from spheroids in cross-linked matrices and alters the resultant angiogenic sprout morphology. Together, these results show that 3D matrix stiffness plays an important role in regulating angiogenesis and vascular stability.

The vasculature within tumors is known to have disrupted cell–cell junctions and to be more permeable than the vasculature in normal tissues (2). Notably, both our current and previous work indicate that matrix stiffness can disrupt VE-cadherin cell–cell junctions and increase vessels' leakiness (20). Interestingly, strong VE-cadherin cell–cell interaction can prevent sprouting (31). In addition, differential VE-cadherin dynamics between cell–cell junctions are required for vascular morphogenesis (32). Expression of the cytoplasmic tail of VE-cadherin can induce endothelial membrane protrusions in a process that depends on its subcellular localization (33). Taken together, these observations highlight a possible links among matrix stiffness, VE-cadherin localization, vessel leakiness, and sprouting dynamics.

Increased matrix density is known to act as a barrier to cell migration (13, 14), and any effect from increased stiffness caused by increased density cannot be decoupled from the altered matrix architecture. Others have demonstrated transient, decreased sprouting responses in matrices glycated with glucose-6-phospate but also noted increased branching and tortuosity (34, 35). Of note, direct exposure to high concentrations of glucose is known to affect cells adversely (36), whereas AGEs can have direct antiangiogenic effects on ECs (37, 38). Interestingly, it has been suggested that AGEs could contribute to ECM stiffening in tumors (29). In our experiments, increasing the collagen matrix stiffness via a preglycation step results in more angiogenic sprouting in vitro and *ex ovo*. Moreover, inhibition of the cross-linking in tumors in vivo resulted in reduced vasculature density and permeability. Such findings are consistent with the decreased rate of metastasis observed in BAPN-treated mice (39), suggesting lower vasculature density and permeability could reduce the ability of tumor cells to enter the blood stream. Furthermore, alternative methods of increasing collagen matrix stiffness, such as the use of microbial transglutaminase or varying the ratio of collagen monomers to oligomers, support our findings of increased angiogenic outgrowth in stiffer matrices (40, 41). Overall, when combined with our data showing the absence of increased endothelial permeability strictly resulting from collagen glycation, these findings indicate that matrix stiffness acts as an important regulator of the vascular phenotype.

Previously published work has shown that MMP activity is an important regulator of angiogenesis (10, 42, 43). GM6001 is a broad-spectrum MMP inhibitor that is known to inhibit the degradation of collagen by MMPs and, interestingly, has been shown to reduce the formation of angiogenic structures in response to the matrix density of fibrin gels (10). Prior studies have seen differences in the angiogenic sprouting response following extended incubation times (3–21 d) with different GM6001 concentrations and collagen matrix density (10, 42, 43). Similarly, we demonstrate that MMP activity is essential for the increased angiogenic response we observed within the stiffer, cross-linked collagen gels. Importantly, both the amount of active cleaved fragment of MT1-MMP and the total content were significantly higher in stiffer matrix. The GM6001 treatment resulted in a small decrease in angiogenic sprouting (along with dramatic changes in the sprout morphology) after 3 d of culture in the compliant collagen gels, whereas GM6001 treatment completely blocked the stiffness-mediated angiogenesis in the *ex ovo* CAM model. Taken together, these data show that MMPs are integral to the formation of angiogenic sprouts occurring in stiffer matrix.

Antiangiogenic therapies targeting VEGF are currently in therapeutic use and do provide some benefit (3, 44). However, although such therapeutics strategies are effective on a short time scale, they do not completely block the angiogenic process or provide sustained long-term normalization of the tumor vasculature (3, 45). Interestingly, these treatments induce severe tumor hypoxia (46). In turn, hypoxia has been shown to promote ECM remodeling and the expression of cross-linking proteins such as LOX (47, 48). Therefore, our current results provide a potential explanation for why increasing matrix stiffness promotes tumor revascularization. Increased matrix stiffness has been shown to potentiate cell responses to several different soluble factors present in the tumor microenvironment (49–51), and in some cases increased matrix stiffness can change the signaling pathways triggered by soluble factors (50). Thus it is possible that the interplay between matrix stiffness and soluble factors might induce or even worsen the tumor-like vascular phenotype. Overall, a combined therapeutics strategy that includes targeting matrix stiffness or the cellular response to stiffness is likely to improve the outcome of primary treatments targeting angiogenic factors or other soluble factors.

Overall, increasing matrix stiffness promotes a tumor-like vascular phenotype, most notably by disrupting vessel architecture and integrity and promoting outgrowth. The altered vascular phenotype promoted by altered stiffness most likely involves the interplay between cell contractility and matrix stiffness. Notably, similar to our findings in ECs, activation of MT1-MMP in epithelial cells depends on both matrix stiffness and cell contractility (24). In addition, both the angiogenic process and tumor permeability are regulated by VEGF receptors, which in turn are known to be transactivated by integrin receptors (52, 53). Interestingly, alternative splicing of protein isoforms, including VEGF and proangiogenic signaling proteins, is regulated by matrix stiffness (22). Therefore, our results show that a further understanding of the underlying mechanism governing the relationship between matrix stiffness and tumor vascular phenotype is needed to design therapeutics targeting either tumor stiffness or the EC response to tumor stiffening.

Materials and Methods

All mice were maintained following a protocol approved by the Cornell University Institutional Animal Care and Use Committee. A detailed description of the protocols used in this study, including mice and chicks studies, cell culture, spheroid generation and studies, Western blotting, immunofluorescence, permeability assays, confocal reflectance imaging, single-cell migration, PA gel

synthesis, and the preparation of collagen scaffolds are described in *SI Materials and Methods*.

ACKNOWLEDGMENTS. This work was supported in part by NIH Grant R01-HL127499 (to C.A.R.-K.), National Science Foundation (NSF) awards 1055502 and 1435755 (to C.A.R.-K.), and NIH Grant R01-CA163255 (to R.S.W.). F.B. is the recipient of a Scholarship for the Next Generation of Scientists from the Cancer Research Society. B.N.M. is the recipient of an NSF Graduate Research Fellowship in Science, Technology, Engineering and Mathematics, The Morgan Family Fellowship, and an NSF Graduate Teaching Fellows in K-12 Education Fellowship. Y.L.N.A. is the recipient of NIH Training Grant T32 GM008500. Imaging data were acquired in the Cornell Biotechnology Resource Center Imaging Facility using the shared, NIH-funded (Grant S10OD016191) VisualSonics high-resolution ultrasound platform and the New York State Stem Cell Science (Grant CO29155)- and NIH (Grant S10OD018516)-funded Zeiss LSM880 confocal/multiphoton microscope.

1. Trédan O, Galmarini CM, Patel K, Tannock IF, Tredan O (2007) Drug resistance and the solid tumor microenvironment. *J Natl Cancer Inst* 99(19):1441–1454.
2. Hashizume H, et al. (2000) Openings between defective endothelial cells explain tumor vessel leakiness. *Am J Pathol* 156(4):1363–1380.
3. Goel S, et al. (2011) Normalization of the vasculature for treatment of cancer and other diseases. *Physiol Rev* 91(3):1071–1121.
4. Carmeliet P (2000) VEGF gene therapy: Stimulating angiogenesis or angioma-genesis? *Nat Med* 6(10):1102–1103.
5. Jain RK (2005) Normalization of tumor vasculature: An emerging concept in anti-angiogenic therapy. *Science* 307(5706):58–62.
6. Levental KR, et al. (2009) Matrix crosslinking forces tumor progression by enhancing integrin signaling. *Cell* 139(5):891–906.
7. Lu P, Weaver VM, Werb Z (2012) The extracellular matrix: A dynamic niche in cancer progression. *J Cell Biol* 196(4):395–406.
8. Maskarinec G, et al. (2013) Mammographic density as a predictor of breast cancer survival: The multiethnic cohort. *Breast Cancer Res* 15(1):R7.
9. Barker HE, et al. (2011) LOXL2-mediated matrix remodeling in metastasis and mammary gland involution. *Cancer Res* 71(5):1561–1572.
10. Ghajar CM, Blevins KS, Hughes CC, George SC, Putnam AJ (2006) Mesenchymal stem cells enhance angiogenesis in mechanically viable prevascularized tissues via early matrix metalloproteinase upregulation. *Tissue Eng* 12(10):2875–2888.
11. Shen CJ, et al. (2011) Decreased cell adhesion promotes angiogenesis in a Pyk2-dependent manner. *Exp Cell Res* 317(13):1860–1871.
12. Cross VL, et al. (2010) Dense type I collagen matrices that support cellular remodeling and microfabrication for studies of tumor angiogenesis and vasculogenesis in vitro. *Biomaterials* 31(33):8596–8607.
13. Edgar LT, Underwood CJ, Guilkey JE, Hoying JB, Weiss JA (2014) Extracellular matrix density regulates the rate of neovessel growth and branching in sprouting angiogenesis. *PLoS One* 9(1):e85178.
14. Carey SP, Kraning-Rush CM, Williams RM, Reinhart-King CA (2012) Biophysical control of invasive tumor cell behavior by extracellular matrix microarchitecture. *Biomaterials* 33(16):4157–4165.
15. Wolf K, et al. (2013) Physical limits of cell migration: Control by ECM space and nuclear deformation and tuning by proteolysis and traction force. *J Cell Biol* 201(7):1069–1084.
16. Chen L, et al. (2014) MT2-MMP expression associates with tumor progression and angiogenesis in human lung cancer. *Int J Clin Exp Pathol* 7(6):3469–3477.
17. Seano G, et al. (2014) Endothelial podosome rosettes regulate vascular branching in tumour angiogenesis. *Nat Cell Biol* 16(10):931–941, 1–8.
18. Ager EI, et al. (2015) Blockade of MMP14 activity in murine breast carcinomas: Implications for macrophages, vessels, and radiotherapy. *J Natl Cancer Inst* 107(4):djv017.
19. Mason BN, Starchenko A, Williams RM, Bonassar LJ, Reinhart-King CA (2013) Tuning three-dimensional collagen matrix stiffness independently of collagen concentration modulates endothelial cell behavior. *Acta Biomater* 9(1):4635–4644.
20. Huynh J, et al. (2011) Age-related intimal stiffening enhances endothelial permeability and leukocyte transmigration. *Sci Transl Med* 3(112):112ra122.
21. Reinhart-King CA, Dembo M, Hammer DA (2008) Cell-cell mechanical communication through compliant substrates. *Biophys J* 95(12):6044–6051.
22. Bordeleau F, et al. (2015) Tissue stiffness regulates serine/arginine-rich protein-mediated splicing of the extra domain B-fibronectin isoform in tumors. *Proc Natl Acad Sci USA* 112(27):8314–8319.
23. Lopez JI, Kang I, You W-KK, McDonald DM, Weaver VM (2011) In situ force mapping of mammary gland transformation. *Integr Biol* 3(9):910–921.
24. Haage A, Schneider IC (2014) Cellular contractility and extracellular matrix stiffness regulate matrix metalloproteinase activity in pancreatic cancer cells. *FASEB J* 28(8):3589–3599.
25. Dvorak HF, Nagy JA, Dvorak JT, Dvorak AM (1988) Identification and characterization of the blood vessels of solid tumors that are leaky to circulating macromolecules. *Am J Pathol* 133(1):95–109.
26. Califano JP, Reinhart-King CA (2010) Substrate Stiffness and Cell Area Predict Cellular Traction Stresses in Single Cells and Cells in Contact. *Cell Mol Bioeng* 3(1):68–75.
27. Califano JP, Reinhart-King CA (2008) A balance of substrate mechanics and matrix chemistry regulates endothelial cell network assembly. *Cell Mol Bioeng* 1(2-3):122–132.
28. van Heijst JWJ, Niessen HWM, Hoekman K, Schalkwijk CG (2005) Advanced glycation end products in human cancer tissues: Detection of Nepsilon-(carboxymethyl)lysine and argpyrimidine. *Ann N Y Acad Sci* 1043:725–733.
29. Rodriguez-Teja M, et al. (2015) AGE-modified basement membrane cooperates with Endo180 to promote epithelial cell invasiveness and decrease prostate cancer survival. *J Pathol* 235(4):581–592.
30. Hirose A, Tanikawa T, Mori H, Okada Y, Tanaka Y (2010) Advanced glycation end products increase endothelial permeability through the RAGE/Rho signaling pathway. *FEBS Lett* 584(1):61–66.
31. Abraham S, et al. (2009) VE-cadherin-mediated cell-cell interaction suppresses sprouting via signaling to MLC2 phosphorylation. *Curr Biol* 19(8):668–674.
32. Bentley K, et al. (2014) The role of differential VE-cadherin dynamics in cell rearrangement during angiogenesis. *Nat Cell Biol* 16(4):309–321.
33. Kouklis P, Konstantoulaki M, Malik AB (2003) VE-cadherin-induced Cdc42 signaling regulates formation of membrane protrusions in endothelial cells. *J Biol Chem* 278(18):16230–16236.
34. Francis-Sedlak ME, et al. (2009) Characterization of type I collagen gels modified by glycation. *Biomaterials* 30(9):1851–1856.
35. Francis-Sedlak ME, et al. (2010) Collagen glycation alters neovascularization in vitro and in vivo. *Microvasc Res* 80(1):3–9.
36. Roy R, Boskey AL, Bonassar LJ (2008) Non-enzymatic glycation of chondrocyte-seeded collagen gels for cartilage tissue engineering. *J Orthop Res* 26(11):1434–1439.
37. Zhou Z, et al. (2012) The Akt-SRPK-SR axis constitutes a major pathway in transducing EGF signaling to regulate alternative splicing in the nucleus. *Mol Cell* 47(3):422–433.
38. Stirban A, Gawlowski T, Roden M (2013) Vascular effects of advanced glycation endproducts: Clinical effects and molecular mechanisms. *Mol Metab* 3(2):94–108.
39. Le Q-T, et al. (2009) Validation of lysyl oxidase as a prognostic marker for metastasis and survival in head and neck squamous cell carcinoma: Radiation Therapy Oncology Group trial 90-03. *J Clin Oncol* 27(26):4281–4286.
40. Lee P-F, Bai Y, Smith RL, Bayless KJ, Yeh AT (2013) Angiogenic responses are enhanced in mechanically and microscopically characterized, microbial transglutaminase cross-linked collagen matrices with increased stiffness. *Acta Biomater* 9(7):7178–7190.
41. Whittington CF, Yoder MC, Voytik-Harbin SL (2013) Collagen-polymer guidance of vessel network formation and stabilization by endothelial colony forming cells in vitro. *Macromol Biosci* 13(9):1135–1149.
42. Bayless KJ, Davis GE (2003) Sphingosine-1-phosphate markedly induces matrix metalloproteinase and integrin-dependent human endothelial cell invasion and lumen formation in three-dimensional collagen and fibrin matrices. *Biochem Biophys Res Commun* 312(4):903–913.
43. Saunders WB, et al. (2006) Coregulation of vascular tube stabilization by endothelial cell TIMP-2 and pericyte TIMP-3. *J Cell Biol* 175(1):179–191.
44. Ribatti D (2016) Tumor refractoriness to anti-VEGF therapy. *Oncotarget* 7(29):46668–46677.
45. Allen E, Walters IB, Hanahan D (2011) Brivanib, a dual FGF/VEGF inhibitor, is active both first and second line against mouse pancreatic neuroendocrine tumors developing adaptive/evasive resistance to VEGF inhibition. *Clin Cancer Res* 17(16):5299–5310.
46. Pàez-Ribes M, et al. (2009) Antiangiogenic therapy elicits malignant progression of tumors to increased local invasion and distant metastasis. *Cancer Cell* 15(3):220–231.
47. Erler JT, et al. (2006) Lysyl oxidase is essential for hypoxia-induced metastasis. *Nature* 440(7088):1222–1226.
48. Gilkes DM, Bajpai S, Chaturvedi P, Wirtz D, Semenza GL (2013) Hypoxia-inducible factor 1 (HIF-1) promotes extracellular matrix remodeling under hypoxic conditions by inducing P4HA1, P4HA2, and PLOD2 expression in fibroblasts. *J Biol Chem* 288(15):10819–10829.
49. Huynh J, Bordeleau F, Kraning-Rush CM, Reinhart-King CA (2013) Substrate stiffness regulates PDGF-induced circular dorsal ruffle formation through MLCK. *Cell Mol Bioeng* 6(2):138–147.
50. Leight JL, Wozniak MA, Chen S, Lynch ML, Chen CS (2012) Matrix rigidity regulates a switch between TGF-β1-induced apoptosis and epithelial-mesenchymal transition. *Mol Biol Cell* 23(5):781–791.
51. Kim JH, Asthagiri AR (2011) Matrix stiffening sensitizes epithelial cells to EGF and enables the loss of contact inhibition of proliferation. *J Cell Sci* 124(Pt 8):1280–1287.
52. Lamalice L, Le Boeuf F, Huot J (2007) Endothelial cell migration during angiogenesis. *Circ Res* 100(6):782–794.
53. Lichtenbeld HC, Ferarra N, Jain RK, Munn LL (1999) Effect of local anti-VEGF antibody treatment on tumor microvessel permeability. *Microvasc Res* 57(3):357–362.
54. Yalcin HC, Shekhar A, Rane AA, Butcher JT (2010) An ex-ovo chicken embryo culture system suitable for imaging and microsurgery applications. *J Vis Exp* (44):2154.
55. Nguyen M, Shing Y, Folkman J (1994) Quantitation of angiogenesis and antiangiogenesis in the chick embryo chorioallantoic membrane. *Microvasc Res* 47(1):31–40.
56. Galli M, Comley KSCC, Shean TAVV, Oyen ML (2009) Viscoelastic and poroelastic mechanical characterization of hydrated gels. *J Mater Res* 24(3):973–979.
57. Hoffmann A, et al. (2011) High and low molecular weight fluorescein isothiocyanate (FITC)-dextrans to assess blood-brain barrier disruption: Technical considerations. *Transl Stroke Res* 2(1):106–111.
58. Machon C, et al. (2014) Quantification of β-aminopropionitrile, an inhibitor of lysyl oxidase activity, in plasma and tumor of mice by liquid chromatography tandem mass spectrometry. *Biomed Chromatogr* 28(7):1017–1023.
59. Lampugnani MG, et al. (1995) The molecular organization of endothelial cell to cell junctions: Differential association of plakoglobin, beta-catenin, and alpha-catenin with vascular endothelial cadherin (VE-cadherin). *J Cell Biol* 129(1):203–217.